

MEASURING ANGULAR DIAMETER DISTANCES THROUGH HALO CLUSTERING

ASANTHA COORAY,^{1,2} WAYNE HU,¹ DRAGAN HUTERER,³ AND MICHAEL JOFFRE¹

Received 2001 May 7; accepted 2001 July 13; published 2001 July 20

ABSTRACT

Current and upcoming wide-field surveys for weak gravitational lensing and the Sunyaev-Zeldovich effect will generate mass-selected catalogs of dark matter halos with internal or follow-up photometric redshift information. Using the shape of the linear power spectrum as a standard ruler that is calibrated by cosmic microwave background measurements, we find that a survey of 4000 deg² and a mass threshold of 10¹⁴ M_⊙ can be used to determine the comoving angular diameter distance as a function of redshift. In principle, this test also allows an absolute calibration of the distance scale and measurement of the Hubble constant. This test is largely insensitive to the details of halo mass measurements, mass function, and halo bias. Determination of these quantities would further allow a measurement of the linear growth rate of fluctuations.

Subject headings: cosmology: theory — large-scale structure of universe

On-line material: color figures

1. INTRODUCTION

A number of observational efforts are now underway or being planned to image the large-scale structure of the universe spanning a range of redshifts. These wide-field surveys typically cover tens to thousands of square degrees of the sky: the ongoing Sloan Digital Sky Survey, the weak gravitational lensing shear observations with instruments such as the *Supernova/Acceleration Probe (SNAP)* or the Large Aperture Synoptic Survey Telescope, and surveys of the Sunyaev-Zeldovich (SZ) effect (Sunyaev & Zeldovich 1980).

In addition to their primary science goals, these surveys are expected to produce catalogs of dark matter halos, which in the case of lensing and SZ surveys are expected to be essentially mass-selected (Wittman et al. 2001; Holder et al. 2000). Lensing and other optical surveys are particularly promising in that they will provide photometric redshifts on the member galaxies of a given halo (e.g., Hogg et al. 1998); this will render accurate determination of the halo redshift. Halo number counts as a function of redshift is a well-known and powerful cosmological test. Here we consider the additional information supplied by the angular clustering of halos.

A feature in an angular power spectrum of known physical scale and originating from a known redshift can be used to measure the angular diameter distance between us and this redshift; this has most notably been applied to the case of the cosmic microwave background (CMB) to determine the distance to redshift $z \sim 10^3$. The angular power spectrum of halos provides a similar test based on the standard ruler defined by its shape. In the adiabatic cold dark matter (CDM) model for structure formation, this standard ruler is essentially the horizon at matter-radiation equality, and its absolute physical scale can be directly calibrated with CMB anisotropy data. In principle then, one can determine the angular diameter distance as a function of redshift and test the properties of the dark energy.

As a purely geometric test, this method is largely insensitive

to uncertainties in the mass function and the relationship between the halo masses and the actual observables, e.g., the SZ temperature decrement or lensing aperture mass. The bias of the halos is scale-dependent only on small (nonlinear) scales and can, in principle, be extracted to arbitrary precision from N -body simulations. If and when these quantities are securely known, one can extract further information from the amplitude and small-scale behavior of the power spectrum. In particular, the linear growth rate and nonlinear scale provide extra handles on the dark energy.

For illustrative purposes, we adopt the Λ CDM cosmology with energy densities (relative to critical) of $\Omega_m = 0.35$ in matter, $\Omega_b = 0.05$ in baryons, $\Omega_\Lambda = 0.65$ in vacuum energy, the dimensionless Hubble constant of $h = 0.65$, and a scale-invariant spectrum of primordial fluctuations, normalized to the present-day galaxy cluster abundance ($\sigma_8 = 0.9$; Viana & Liddle 1999).

2. ANGULAR POWER SPECTRUM

The angular power spectrum of halos in i th redshift bin is a Limber (1954; Kaiser 1992) projection of the halo number density power spectrum

$$C_i^l = \int dz W_i^2(z) \frac{H(z)}{d_A^2(z)} P_{hh} \left(\frac{l}{d_A}; z \right), \quad (1)$$

where $W_i(z)$ is the distribution of halos in a given redshift bin normalized so that $\int dz W_i(z) = 1$, $H(z)$ is the Hubble parameter, and d_A is the angular diameter distance in comoving coordinates. Note that $W_i(z)$ comes directly from the observations of the number counts as a function of redshift and depends on the mass function and mass sensitivity of the employed observable.

If the halos trace the linear density field,

$$P_{hh}(k; z) = \langle b_M \rangle^2(z) D^2(z) P^{\text{lin}}(k; 0), \quad (2)$$

where $\langle b_M \rangle$ is the mass-averaged halo bias parameter, $P^{\text{lin}}(k; 0)$ is the present-day matter power spectrum computed in linear theory, and $D(z)$ is the linear growth function $\delta^{\text{lin}}(k; z) = D(z)\delta^{\text{lin}}(k; 0)$. A scale-independent halo bias is commonly assumed in the so-called halo model (e.g., Seljak

¹ Department of Astronomy and Astrophysics, University of Chicago, 5640 South Ellis Avenue, Chicago, IL 60637; asante@oddjjob.uchicago.edu, whu@oddjjob.uchicago.edu, joffre@oddjjob.uchicago.edu.

² Sherman Fairchild Senior Research Fellow, Department of Physics, California Institute of Technology, MS 130-33, Pasadena, CA 91125.

³ Department of Physics, University of Chicago, 5640 South Ellis Avenue, Chicago, IL 60637; dhuterer@oddjjob.uchicago.edu.

2000) and should be valid at least in the linear regime. Equation (1) then becomes

$$C_l^i = \int dz W_i^2(z) F(z) P^{\text{lin}}\left(\frac{l}{d_A^i}; 0\right), \quad (3)$$

$$F(z) = \frac{H(z)}{d_A^2(z)} D(z)^2 \langle b_M \rangle^2(z). \quad (4)$$

The underlying linear power spectrum contains two physical scales: the horizon at matter-radiation equality,

$$k_{\text{eq}} = \sqrt{2\Omega_m H_0^2 (1 + z_{\text{eq}})} \propto \Omega_m h^2, \quad (5)$$

which controls the overall shape of the power spectrum, and the sound horizon at the end of the Compton drag epoch, $k_s(\Omega_m h^2, \Omega_b h^2)$, which controls the small wiggles in the power spectrum. The angular or multipole locations of these features shift in redshift as $l_{\text{eq},s} = k_{\text{eq},s} d_A(z_i)$. We propose the following test: measure C_l^i in several redshift bins and, using the fact that l_{eq} scales with $d_A(z_i)$, constrain the angular diameter distance as a function of redshift. To be conservative, we ignore the additional information supplied by l_s .

In Figure 1, we illustrate the proposed test. The two curves show the halo power spectra in two redshift bins: $0.3 < z < 0.4$ and $1.0 < z < 1.2$. The angular power spectrum corresponding to the higher redshift bin is shifted to the right in accordance to the ratio of angular diameter distances ($\delta l/l \sim \delta d_A/d_A$). Much of this shift simply reflects the Hubble law, $d_A \approx z/H_0$. Since the physical scale of the two features—the overall shape of the spectrum and the baryon oscillations—can be calibrated from the morphology of the CMB peaks, these measurements can, in principle, be used to determine the Hubble constant independently of the distance ladder and distance to last scattering surface.

In addition to the horizontal shift due to the change in angular diameter distance, the power spectra in Figure 1 are shifted vertically due to the change in $F(z)$ (eq. [4]). By ignoring the information contained in $F(z)$, this purely geometric test is robust against uncertainties in the mass selection, mass function, and linear bias. Of course, if these uncertainties are pinned down independently, both $F(z)$ and the halo abundance in $W_i(z)$ will help measure the growth rate of structure.

3. PARAMETER ESTIMATION

Even though the angular diameter distance test is robust against uncertainties in the halo selection function, number density, and bias, these quantities enter into the consideration of the signal-to-noise ratio for a realistic survey. We will focus on a survey of 4000 deg^2 with a detection threshold in mass of $10^{14} M_\odot$ out to $z = 2$. We use a total of nine bins in redshift; note that the cluster photometric redshift accuracy is expected to be much smaller than the bin width. The mass threshold is consistent with those expected from upcoming lensing and SZ effect surveys (see Kruse & Schneider 1999; Holder et al. 2000; M. Joffre et al. 2001, in preparation), and the survey area is consistent with a planned SZ survey from the South Pole Telescope (J. E. Carlstrom 2000, private communication). To compute $W_i^2(z)$, we adopt the predictions of the Press-Schechter (PS) mass function (Press & Schechter 1974). This mass function, along with the halo bias prescription of Mo & White (1996), is also used to predict the mass-averaged halo bias $\langle b_M \rangle(z)$.

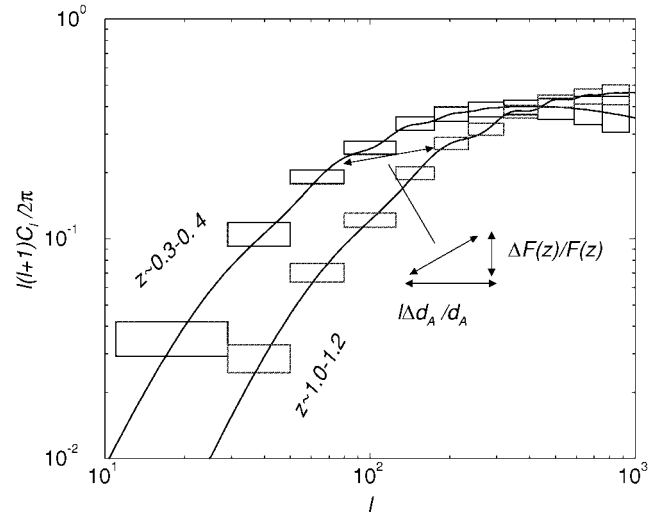


FIG. 1.—Angular power spectrum of halos with $M > 10^{14} M_\odot$ in a wide-field survey in bins of $z = 0.3\text{--}0.4$ and $1.0\text{--}1.2$. The binned errors are 1σ and assume a survey of 4000 deg^2 , within reach of upcoming weak lensing and SZ surveys. The angular power spectrum at high redshifts is shifted toward the right proportional to the increase in the comoving angular diameter distance. The oscillations are due to baryons, but we ignore the additional information they contain. [See the electronic edition of the Journal for a color version of this figure.]

Assuming Gaussian statistics, we can express the uncertainty in the measurements of the angular power spectrum as

$$\Delta C_l^i = \frac{(C_l^i + N_l^i)}{\sqrt{(l+1/2)f_{\text{sky}}}}, \quad (6)$$

where $f_{\text{sky}} = \Theta_{\text{deg}}^2 \pi / 129,600$ is the fraction of the sky covered by a survey of dimension Θ_{deg} in degrees and N_l^i is the noise power spectrum. We assume that the dominant source of noise is the shot noise so that $N_l^i \equiv 1/\bar{N}_l$, where \bar{N}_l is the surface density of the halos in the i th redshift bin. We use the PS mass function to predict \bar{N}_l . In Figure 1, the two bins contain roughly 4 and 6 halos deg^{-2} above our minimum mass. In the same figure, we show band power measurement errors following equation (6).

To estimate how well halo clustering can recover cosmological information, we construct the Fisher matrix,

$$\mathbf{F}_{\alpha\beta} = \sum_{i=1}^{N_{\text{bins}}} \sum_{l=l_{\text{min}}}^{l_{\text{max}}} \frac{(l+1/2)f_{\text{sky}}}{(C_l^i + N_l^i)^2} \frac{\partial C_l^i}{\partial p_\alpha} \frac{\partial C_l^i}{\partial p_\beta}, \quad (7)$$

where α and β label parameters that underly the power spectra. Since the variance of an unbiased estimator of a parameter p_α cannot be less than $(\mathbf{F}^{-1})_{\alpha\alpha}$, the Fisher matrix quantifies the best statistical errors on parameters possible with a given data set.

We choose $l_{\text{min}} = 2\pi/\Theta_{\text{deg}}$ when evaluating equation (7), as it corresponds roughly to the survey size. The precise value does not matter for parameter estimation due to the increase in sample variance on the survey scale. Given our crude Gaussian approximation of the shot noise, we choose a conservative l_{max} corresponding to the multipole at which the noise and sample variances are equal, $N_l^i = C_l^i$; l_{max} ranges from 200 at low-redshift bins to 400 at high redshift. At low redshifts, this cutoff is slightly in the nonlinear regime, but at redshifts greater than 0.8 or so, one is well within the linear regime. Therefore,

such a low l_{\max} largely eliminates uncertainties in the modeling of scale-dependent halo bias in the nonlinear regime.

Due to the dependence of C_i on $P^{\text{lin}}(k)$, all cosmological parameters that change the shape of the matter power spectrum across the scales probed by halos also affect the measurement of distance. The shape of the transfer function is determined by $\Omega_m h^2$ and $\Omega_b h^2$, while the overall slope is determined by a scalar tilt n_s . Note that these parameters will be accurately determined from CMB anisotropy observations. Since the CMB peaks probe the same range in spatial scale as the halo power spectrum, one is relatively insensitive to deviations from a pure initial power law.

When estimating expected errors on distance, we will consider several sets of priors on these cosmological parameters. These priors follow Table 2 of Eisenstein, Hu, & Tegmark (1999) and correspond to constraints expected from the *Microwave Anisotropy Probe (MAP)* and *Planck* with and without polarization. Although baryon oscillations contain cosmological information, in order to be conservative against possible nonlinearities in the bias we ignore the information present in the baryon oscillations and employ the smooth fitting function of Eisenstein & Hu (1999). Our results are then very weakly dependent on the fiducial value or priors on $\Omega_b h^2$. In case baryonic features in the angular power spectrum are detected, we expect additional cosmological information to be gained using the proposed test.

4. RESULTS AND DISCUSSION

We first consider the measurement of the angular diameter distance $d_A^i = d_A(z_i)$. In addition to the cosmological parameters $\Omega_m h^2$, $\Omega_b h^2$, and n_s , we include a set of parameters $F^i = F(z_i)$, which allow the normalization of the i power spectra to float independently. Both d_A^i and F^i approximate underlying functions as piecewise flat across each bin.

In the top panel of Figure 2, we show three sets of errors: the largest errors assume no prior knowledge on the transfer function, while the smaller errors correspond to priors from *MAP* (temperature) and *Planck* (polarization), respectively (Hu et al. 1999). In the bottom panel of Figure 2, we show the fractional percentage errors on the distance. The errors in the lowest bins tell us how well one can estimate the Hubble constant, while the slope of $d_A(z)$ around $z \sim 1$ provides information on cosmology; d_A is best determined around $z \approx 0.7$ at the level of 10%. For systematic errors in the redshifts to dominate the error budget, the inferred mean redshift of the bin must differ from the true value by $\sim 10\%$, which is far above the errors we expect for individual halos even from photometric techniques at $z < 1$. Precision at higher redshift is not required because of the large statistical errors. The errors on distance estimates d_A^i are correlated at the 5% level due to remaining uncertainties in parameters that affect all d_A^i (e.g., $\Omega_m h^2$).

In a realistic cosmology, $d_A(z)$ is smoothly varying. Since $\Omega_m h^2$ is already taken as a parameter, we parameterize d_A with the Hubble constant $h = H_0/100 \text{ km s}^{-1} \text{ Mpc}^{-1}$ and the equation of state of the dark energy w , the ratio of pressure to density, assuming a flat universe. We bin halos following the binning scheme in Figure 2. In the top panel of Figure 3, we show that a strong degeneracy in h and w remains even with *Planck* priors because d_A is accurately recovered only in a small redshift range. Of course, an external determination of h would break this degeneracy.

An alternate way of breaking the degeneracy is to employ other cosmological probes of Ω_m and w . As shown in the bottom

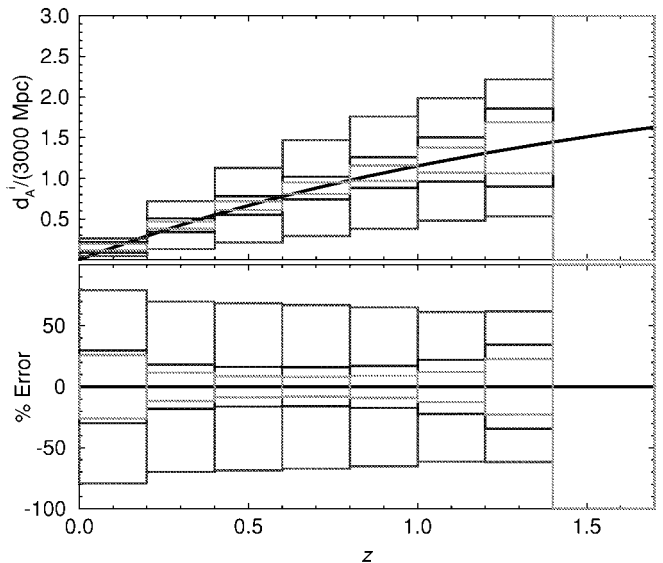


FIG. 2.—*Top*: Errors (1σ) on angular diameter distance as a function of redshift. We have binned the halos in eight redshift bins between 0 and 1.6. The larger errors are with no prior assumption on the cosmological parameters that define the transfer function, while the smaller errors are with *MAP* (temperature) and *Planck* (polarization) priors. *Bottom*: Relative errors in the distance. [See the electronic edition of the *Journal* for a color version of this figure.]

panel of Figure 3, different linear combinations of Ω_m and w will be determined by halos and the CMB due to the different redshift ranges probed. Although each constraint alone may not be able to pin down w , halos and the CMB combined allow very interesting constraints even under our conservative assumptions.

Uncertainties in the mass threshold and the scale dependence of halo bias are potential caveats to these conclusions. A mass threshold that differs from the assumed $10^{14} M_\odot$ value would not bias the angular diameter distance results since they only utilize redshift and power spectrum shape information. However, it would affect the errors due to a rapid decrease in the number density of halos with threshold mass: at $4 \times 10^{14} M_\odot$, the error on w increases by a factor of ~ 3 .

A scale-dependent bias that can be predicted actually aids in the determination of angular diameter distances; the scale dependence acts as another standardizable ruler for the test. Indeed, the scale dependence of the bias as a function of halo mass is something that can be precisely determined from N -body simulations (Kravtsov & Klypin 1999). A more subtle problem is introduced by the addition of uncertainties in the mass threshold or selection function. Since the bias is also mass-dependent, the uncertainty in the mass threshold $\delta M/M = 0.1$ translates into the uncertainty in the mass-averaged bias $\delta \langle b_M \rangle / \langle b_M \rangle = 0.03$. To investigate a scale-dependent bias, we model it as

$$b_M(k, z) = \langle b_M \rangle(z) \left\{ 1 + f \left[\sqrt{\frac{P^{\text{nl}}(k; z)}{P^{\text{lin}}(k; z)}} - 1 \right] \right\}, \quad (8)$$

where f is a dimensionless parameter meant to interpolate bias between the linear ($f \rightarrow 0$) and the nonlinear ($f \rightarrow 1$) regimes. Note that in the halo approach to clustering, the nonlinear mass power spectrum is a sum of the halo power spectrum and contributions due to dark matter within halos; therefore, the halo power spectrum cannot be larger than the nonlinear power

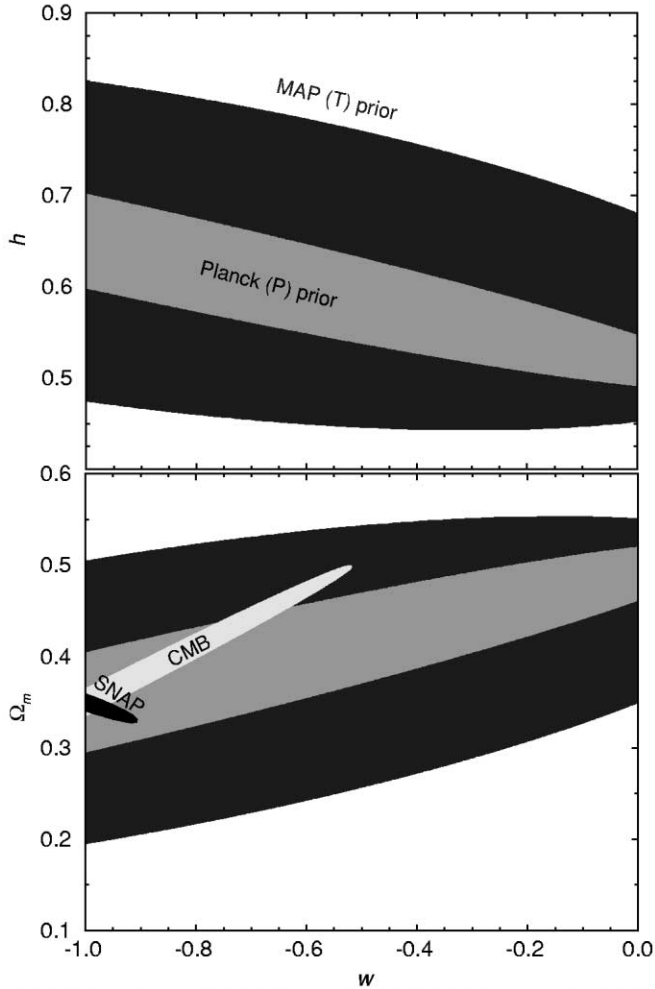


FIG. 3.—Errors (all 1σ) on h and w (top) and Ω_m and w (bottom), using distance information only. In both panels, we show errors for halos with priors following *MAP* (temperature) and *Planck* (polarization). In the bottom panel, for comparison, we also show errors on Ω_m and w from CMB (*Planck* with temperature and polarization [Hu et al. 1999]) and Type Ia supernovae with the *SNAP* mission. [See the electronic edition of the *Journal* for a color version of this figure.]

spectrum. Taking a fiducial model with $f = 0$ and adopting *MAP* (temperature) priors, we find that marginalizing over f increases the error on w by less than 10%.

To the extent that the mass threshold, halo bias, and mass function are known, the amplitude of the halo power spectra can be used to measure the linear growth rate. We conclude by estimating the level at which these quantities must be determined to yield additional constraints on w . In Figure 4, we

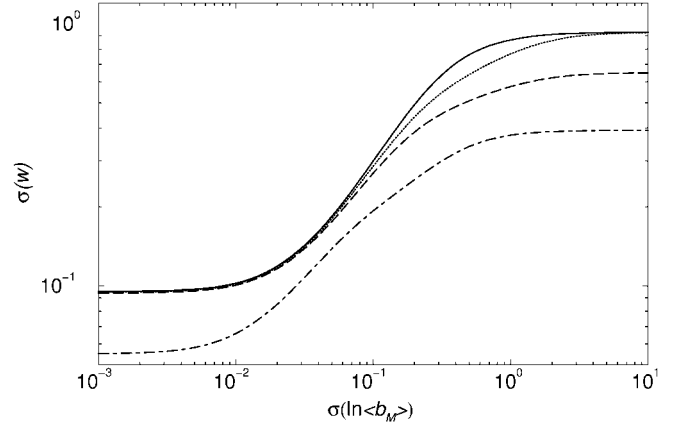


FIG. 4.—The 1σ error on w as a function of the prior on bias. The four curves assume *Planck* (polarization) priors on $\Omega_m h^2$, n_s , and $\Omega_b h^2$ to define the linear power spectrum. The solid line is with no prior on $\ln A$ and h . The dotted line includes a prior of 0.2 in $\ln A$, while the dashed line is with an additional prior of 0.1 in h . The dot-dashed line is a highly optimistic scenario with exact A , a prior of 0.1 in h , and using halo angular power spectrum information out to l_{\max} of 1000, deeply within the nonlinear regime.

plot the marginalized errors on w as a function of the assumed fractional prior on $\langle b_M^i \rangle$ for various independent constraints on A and h . Since cosmological information captured in linear growth is determined by relative amplitude variations in C_i^i , the knowledge of the overall normalization A is not crucial. For example, going from no prior knowledge of A to a Gaussian prior with width of 20% of the fiducial value of A results in a decrease in $\sigma(w)$ of $\sim 25\%$. Errors on the mass selection function bias the measure of w . Using an extension to the Fisher matrix approach, we determined that a 25% systematic offset in mass threshold from the fiducial value of $10^{14} M_\odot$ leads to systematic bias in w of 0.05 from its fiducial value of -1.0 . Lensing simulations (Metzler et al. 1999; Reblinsky & Bartlemann 1999) indicate that the calibration of projection effects at this level will be challenging but feasible to achieve.

Clearly, future surveys that can identify dark matter halos as a function of redshift contain valuable information beyond the evolution of their number abundance. As the theoretical modeling of the halo distribution and empirical modeling of the selection process improve, the correlation function of the halos can provide not only the angular diameter distance but also direct measurements of the growth of large-scale structure.

A. C. and W. H. were supported by NASA grant NAG5-10840 and the Department of Energy (DOE) OJI. D. H. was supported by the DOE. M. J. was supported by NASA grant NAG5-7986.

REFERENCES

- Eisenstein, D. J., & Hu, W. 1999, *ApJ*, 511, 5
 Eisenstein, D. J., Hu, W., & Tegmark, M. 1999, *ApJ*, 518, 2
 Hogg, D. W., et al. 1998, *AJ*, 115, 1418
 Holder, G. P., Mohr, J. J., Carlstrom, J. E., Evrard, A. E., & Leitch, E. M. 2000, *ApJ*, 544, 629
 Hu, W., Eisenstein, D. J., Tegmark, M., & White, M. 1999, *Phys. Rev. D*, 59, 023512
 Kaiser, N. 1992, *ApJ*, 388, 272
 Kravtsov, A. V., & Klypin, A. A. 1999, *ApJ*, 520, 437
 Kruse, G., & Schneider, P. 1999, *MNRAS*, 302, 821
 Limber, D. 1954, *ApJ*, 119, 655
 Metzler, C. A., White, M., Norman, M., & Loken, C. 1999, *ApJ*, 520, L9
 Mo, H. J., & White, S. D. M. 1996, *MNRAS*, 282, 347
 Press, W. H., & Schechter, P. 1974, *ApJ*, 187, 425
 Reblinsky, K., & Bartlemann, M. 1999, *A&A*, 345, 1
 Seljak, U. 2000, *MNRAS*, 318, 203
 Sunyaev, R. A., & Zeldovich, Ya. B. 1980, *MNRAS*, 190, 413
 Viana, P. T. P., & Liddle, A. R. 1999, *MNRAS*, 303, 535
 Wittman, D., Tyson, J. A., Margoniner, V. E., Cohen, J. G., & Dell'Antonio, I. P. 2001, *ApJ*, submitted (astro-ph/0104094)